Frontiers of Information Technology & Electronic Engineering
www.jzus.zju.edu.cn; engineering.cae.cn; www.springerlink.com
ISSN 2095-9184 (print); ISSN 2095-9230 (online)
E-mail: jzus@zju.edu.cn

Hohmann transfer via constrained optimization*

Li XIE‡[1], Yi-qun ZHANG[2], Jun-yan XU[2]

[1]*State Key Laboratory of Alternate Electrical Power System with Renewable Energy Sources, School of Control and Computer Engineering, North China Electric Power University, Beijing 102206, China*

[2]*Beijing Institute of Electronic Systems Engineering, Beijing 100854, China*

E-mail: lixie@ncepu.edu.cn; yiqunzhang@hotmail.com; junyan_Xu@sina.cn

Received May 11, 2018; Revision accepted July 23, 2018; Crosschecked Nov. 27, 2018

Abstract: Inspired by the geometric method proposed by Jean-Pierre MAREC, we first consider the Hohmann transfer problem between two coplanar circular orbits as a static nonlinear programming problem with an inequality constraint. By the Kuhn-Tucker theorem and a second-order sufficient condition for minima, we analytically prove the global minimum of the Hohmann transfer. Two sets of feasible solutions are found: one corresponding to the Hohmann transfer is the global minimum and the other is a local minimum. We next formulate the Hohmann transfer problem as boundary value problems, which are solved by the calculus of variations. The two sets of feasible solutions are also found by numerical examples. Via static and dynamic constrained optimizations, the solution to the Hohmann transfer problem is re-discovered, and its global minimum is analytically verified using nonlinear programming.

Key words: Hohmann transfer; Nonlinear programming; Constrained optimization; Calculus of variations
https://doi.org/10.1631/FITEE.1800295 **CLC number:** O232; V412.4

1 Introduction

In 1925, Dr. Hohmann, a civil engineer, published his seminal book (Hohmann, 1960), in which he first described the well-known optimal orbital transfer between two circular coplanar space orbits by numerical examples, and this transfer is now generally called the Hohmann transfer. Hohmann claimed that the minimum-fuel impulsive transfer orbit is an elliptic orbit tangent to both the initial and final circular orbits. The idea of the tangent-impulse transfer conceived by Hohmann has been used to solve more complicated space transfer problems (Zhang et al., 2014). A mathematical proof to its optimality was not addressed until the 1960s. Ting (1960) considered the local optimality of generalized Hohmann transfers. Barrar (1963) proposed an analytic proof; see also references therein.

Pontani (2009) reviewed the literature concerning the optimality of the Hohmann transfer from the 1970s to the 1990s. Marec (1979) showed a geometric method in view of a hodograph plane. Based on Green's theorem, Hazelrigg (1984) established optimal impulsive transfers. Palmore (1984) provided an elemental proof with the help of the gradient of the characteristic velocity. Battin (1987) considered the Hohmann transfer as a nonlinear optimization problem with equality constraints, and a Lagrange multiplier method was used. Prussing (1992) simplified Palmore's method by using the partial derivatives of the characteristic velocity. Yuan and Matsushima (1995) carefully used two lower bounds of velocity changes for orbital transfers and showed that the Hohmann transfer is optimal in both total velocity change and each velocity change. We note that

‡ Corresponding author

* Project supported by the National Natural Science Foundation of China (No. 61374084)

ORCID: Li XIE, http://orcid.org/0000-0002-5214-9769

a similar argument to Prussing (1992) appeared in Vertregt (1958), which was summarized in Cornelisse et al. (1979).

In the Chinese literature, the issue of optimal orbital transfers was also addressed (Yu, 1990; Li and Li, 1991); in particular, in Li and Li (1991), the optimality of the Hohmann transfer was established by using nonlinear programming with inequality constraints on perigee and apogee radii. These inequality constraints were used in Vertregt (1958), Cornelisse et al. (1979), and Prussing (1992).

Miele et al. (2004) considered the optimality of the Hohmann transfer using nonlinear optimization with equality constraints associated with the energy and angular momentum; see also Mathwig (2004). Recently, Gurfil and Seidelmann (2016) considered the effects of the Earth's oblateness J_2 on the Hohmann transfer. By using Lagrange multipliers, the optimal impulsive transfer has been derived. This transfer is referred to as the extended Hohmann transfer, which degenerates to the standard Hohmann transfer as $J_2 = 0$. Avendaño et al. (2016) presented a pure algebraic approach to the minimum-cost multi-impulse orbit-transfer problem. By using Lagrange multipliers, as a particular example, the optimality of the Hohmann transfer has also been shown by this algebraic approach. These authors are all devoted to proving the optimality of the Hohmann transfer but without considering its global minimum.

In Section 2, we present a different method to prove the global optimality of the Hohmann transfer, from which the global minimum of the Hohmann transfer easily follows. Inspired by the geometric method in Marec (1979), we transform the Hohmann transfer problem into a nonlinear programming problem with an inequality constraint, and then using the results in nonlinear programming such as the well-known Kuhn-Tucker theorem and a second-order sufficient condition for minima, we analytically prove the global minimum of the Hohmann transfer. Two sets of feasible solutions are found: one corresponding to the Hohmann transfer is the global minimum and the other is a local minimum. The orbital transfer pushed by the local minimum is opposite to the Hohmann transfer.

It is known that orbital transfer problems can be formulated as dynamic optimization problems, which can be solved by the calculus of variations. Lawden (1963) used variational methods to investigate the dynamic optimization problem of a spacecraft in an inverse square law field, and invented the primer vector methodology. According to different thrusts, the trajectory of a spacecraft is divided into the arcs of three types: (1) null thrust arc, (2) maximum thrust arc, and (3) intermediate arc. If we approximate the maximum thrust by an impulse thrust, then orbital transfer problems can be studied by the primer vector theory. These are therefore called impulsive transfers, and the Hohmann transfer is a special case. Lawden (1963) also derived all necessary conditions that the primer vector must satisfy. A systemic design instruction can be found in Prussing (2010). For N-impulse coplanar orbital transfers, Moyer (1965) verified the techniques devised individually by Breakwell and Constensou via variational methods. Compared to the dynamic equation for position and velocity vectors in Lawden (1963), the dynamic equation involved was established for orbital elements.

Instead of the static optimization problem, in Section 3, we consider the Hohmann transfer problem as dynamic optimization problems with equality constraints, one of which has an unspecified final time and the other has interior point constraints with a known final time. Then using variational methods, the related dynamic optimization problems are converted into two-point and multi-point boundary-value problems. Boundary conditions (BCs) are derived in terms of the primer vector and the position costate.

In Section 4, three numerical examples are used to demonstrate the theoretical results of static and dynamic optimizations. With the help of Matlab boundary value solvers, the Hohmann transfer is solved from these constrained dynamic optimization problems. With different initial values, the local minimum given by static optimization also appears. The numerical solutions show that the variational method as an indirect optimization method provides highly accurate solutions by using Matlab boundary value solvers once the solutions are found by trial and error.

By formulating the Hohmann transfer problem as static and dynamic constrained optimization problems, the solution to the Hohmann transfer problem is re-discovered and its global minimum is analytically verified.

2 Optimality of the Hohmann transfer

The Hohmann transfer is a two-impulse orbital transfer from one circular orbit to another; for the background, see, e.g., Marec (1979), Prussing and Conway (1993), Curtis (2014), and Longuski et al. (2014). We use the same notation as in Marec (1979). Let O_0 denote the initial circular orbit of a spacecraft, and the radius and the velocity of the initial circular orbit are r_0 and V_0, respectively. Let O_f denote the final circular orbit, and its radius and velocity are r_f and V_f, respectively. For simplicity, let r_f be greater than r_0. We use boldface to denote vectors. The center of these two coplanar circular orbits is at the origin of the Cartesian inertial reference coordinate system. Suppose all transfer orbits are coplanar to O_0 for simplicity. An extension to the three-dimensional (3D) case is also considered in the sequel. Hence, we need only to consider the $x-y$ plane of the reference coordinate system. Assume that the spacecraft is initially located at the point $(r_0,0)$ of the initial circular orbit. At the initial time t_0, the first velocity impulse vector $\Delta\boldsymbol{V}_0$ is applied, and its components in the direction of the radius and the direction perpendicular to the radius (cross-radial direction) are ΔX_0 and ΔY_0, respectively. Similarly, at the final time t_f, the second velocity impulse $\Delta\boldsymbol{V}_\mathrm{f}$ occurs, and its components are ΔX_f and ΔY_f. Hence, at the time t_0^+ just after t_0, the components of the velocity of the spacecraft are $(\Delta X_0, V_0+\Delta Y_0)$. Then to enter the final circular orbit, the components of the velocity of the spacecraft must be $(-\Delta X_\mathrm{f}, V_\mathrm{f}-\Delta Y_\mathrm{f})$ at the time t_f^- just before t_f.

During the period from t_0^+ to t_f^-, the spacecraft is on a transfer orbit (conic) and the angular momentum h and the energy (per unit mass) $\mathcal{E}$ are conserved; hence, we have

$$\begin{aligned} h &= r_0(V_0+\Delta Y_0) = r_\mathrm{f}(V_\mathrm{f}-\Delta Y_\mathrm{f}),\\ \mathcal{E} &= \frac{1}{2}\left[(V_0+\Delta Y_0)^2+\Delta X_0^2\right]-\frac{\mu}{r_0}\\ &= \frac{1}{2}\left[(V_\mathrm{f}-\Delta Y_\mathrm{f})^2+\Delta X_\mathrm{f}^2\right]-\frac{\mu}{r_\mathrm{f}}. \end{aligned} \tag{1}$$

Note that for a circular orbit, its radius and velocity satisfy $V=\sqrt{\mu/r}$ and μ is the gravitational constant. It follows from Eq. (1) that we can express ΔX_0 and ΔY_0 in terms of ΔX_f and ΔY_f, and vice versa. To simplify equations, first, using the initial orbit radius and velocity as reference values, we define new variables as follows:

$$\begin{aligned} &\bar{r}_\mathrm{f}=\frac{r_\mathrm{f}}{r_0}, \quad v_\mathrm{f}=\frac{V_\mathrm{f}}{V_0}, \quad y_0=\frac{\Delta Y_0}{V_0},\\ &x_0=\frac{\Delta X_0}{V_0}, \quad y_\mathrm{f}=\frac{\Delta Y_\mathrm{f}}{V_0}, \quad x_\mathrm{f}=\frac{\Delta X_\mathrm{f}}{V_0}. \end{aligned} \tag{2}$$

Substituting Eq. (2) into Eq. (1) yields the following non-dimensional angular momentum and energy equalities (Marec, 1979):

$$\begin{aligned} h &= (1+y_0)=\bar{r}_\mathrm{f}(v_\mathrm{f}-y_\mathrm{f}),\\ \mathcal{E} &= \frac{1}{2}\left[(1+y_0)^2+x_0^2\right]-1\\ &= \frac{1}{2}\left[(v_\mathrm{f}-y_\mathrm{f})^2+x_\mathrm{f}^2\right]-\frac{1}{\bar{r}_\mathrm{f}}. \end{aligned}$$

Then we express x_f and y_f in terms of x_0 and y_0 as follows:

$$y_\mathrm{f}=v_\mathrm{f}-(1+y_0)\bar{r}_\mathrm{f}^{-1}=\bar{r}_\mathrm{f}^{-1/2}-(1+y_0)\bar{r}_\mathrm{f}^{-1}, \tag{3}$$

$$\begin{aligned} x_\mathrm{f}^2 &= x_0^2+(1+y_0)^2-2(1-\bar{r}_\mathrm{f}^{-1})-(v_\mathrm{f}-y_\mathrm{f})^2\\ &= x_0^2+(1+y_0)^2(1-\bar{r}_\mathrm{f}^{-2})-2(1-\bar{r}_\mathrm{f}^{-1}), \end{aligned} \tag{4}$$

from which we have

$$\begin{aligned} \Delta v_\mathrm{f}^2 &= \left(\frac{\Delta V_\mathrm{f}}{V_0}\right)^2=x_\mathrm{f}^2+y_\mathrm{f}^2\\ &= x_0^2+(1+y_0)^2(1-\bar{r}_\mathrm{f}^{-2})-2(1-\bar{r}_\mathrm{f}^{-1})\\ &\quad+\left(\bar{r}_\mathrm{f}^{-1/2}-(1+y_0)\bar{r}_\mathrm{f}^{-1}\right)^2\\ &= x_0^2+\left(y_0+1-\bar{r}_\mathrm{f}^{-3/2}\right)^2\\ &\quad-(\bar{r}_\mathrm{f}-1)(2\bar{r}_\mathrm{f}^2-\bar{r}_\mathrm{f}-1)\bar{r}_\mathrm{f}^{-3}\\ &= x_0^2+\left(y_0+1-\bar{r}_\mathrm{f}^{-3/2}\right)^2-(\bar{r}_\mathrm{f}-1)^2(2\bar{r}_\mathrm{f}+1)\bar{r}_\mathrm{f}^{-3}, \end{aligned} \tag{5}$$

$$\Delta v_0^2=x_0^2+y_0^2,$$

where we define $\Delta v_0=\sqrt{x_0^2+y_0^2}>0$ and $\Delta v_\mathrm{f}=\sqrt{x_\mathrm{f}^2+y_\mathrm{f}^2}>0$. Thus, the cost function (i.e., the characteristic velocity) can be written as

$$\begin{aligned} \Delta v(x_0,y_0) &= \Delta v_0+\Delta v_\mathrm{f}=\sqrt{x_0^2+y_0^2}\\ &+\sqrt{x_0^2+\left(y_0+1-\bar{r}_\mathrm{f}^{-3/2}\right)^2-(\bar{r}_\mathrm{f}-1)^2(2\bar{r}_\mathrm{f}+1)\bar{r}_\mathrm{f}^{-3}}. \end{aligned}$$

The above background can be found in Marec (1979) which is specified here.

Observing Eq. (4), it is noted that we must make the following constraint on the first impulse:

$$x_0^2+(1+y_0)^2(1-\bar{r}_\mathrm{f}^{-2})-2(1-\bar{r}_\mathrm{f}^{-1})\geq 0. \tag{6}$$

That is, when we use energy conservation to calculate the non-dimensional component of the second impulse x_f, inequality (6) must hold such that a non-negative number is assigned to x_f^2, which actually requires that the transfer orbit intersect the inner circle and the outer circle.

Marec (1979) used the independent variables x_0 and y_0 as coordinates in a hodograph plan and in geometric language, an elegant and simple proof was given to show the optimality of the Hohmann transfer. Marec's geometric method encourages us to consider the Hohmann transfer in a different way. We formulate the Hohmann transfer problem as a nonlinear programming problem subject to inequality constraint (6), in which x_0 and y_0 are independent variables. Then the global minimum of the Hohmann transfer analytically appears.

Theorem 1 For the constrained optimization problem

$$\begin{aligned}&\min_{x_0,y_0}\ \Delta v(x_0,y_0) \qquad (7)\\ &\text{s.t. } x_0^2+(1+y_0)^2(1-\bar{r}_\mathrm{f}^{-2})-2(1-\bar{r}_\mathrm{f}^{-1})\geq 0,\end{aligned}$$

there are two sets of feasible solutions, one of which corresponds to the Hohmann transfer and is the global minimum, and the other is a local minimum.

Before proving Theorem 1, we show that the constrained optimization problem (7) has a global minimum since a coercive function always attains a global minimum on any closed set.

Lemma 1 The cost function $\Delta v(x_0,y_0)$ is a continuous and coercive function and has a global minimum over the constraint set M defined by inequality (6).

Proof Denote $\boldsymbol{x}=[x_0,y_0]^\mathrm{T}$ and $\|\boldsymbol{x}\|=\sqrt{x_0^2+y_0^2}$. Since $\Delta v(x_0,y_0)\geq\sqrt{x_0^2+y_0^2}$, we have

$$\lim_{\|\boldsymbol{x}\|\to\infty}\Delta v(x_0,y_0)=\infty.$$

Therefore, the underlying continuous cost function $\Delta v(x_0,y_0)$ is a coercive function; e.g., see Güler (2010). It is clear that the constraint set M is closed, and hence this lemma is a direct application of Collorary 2.5 in Güler (2010).

We divide the proof of Theorem 1 into the following three steps. By using the first-order necessary condition, two groups of feasible solutions as candidates for local minimum points to problem (7) are found. Then by the second-order sufficient condition, we show that they are strict local minima. Finally, by comparing them and using Lemma 1, one of them corresponding to the Hohmann transfer is the global minimum.

Proof (of Theorem 1) Define an open set as follows:

$$\begin{aligned}O=&\{(x_0,y_0):\Delta v_\mathrm{f}^2=x_0^2+\left(y_0+1-\bar{r}_\mathrm{f}^{-3/2}\right)^2\\&-(\bar{r}_\mathrm{f}-1)^2(2\bar{r}_\mathrm{f}+1)\bar{r}_\mathrm{f}^{-3}>0\}. \qquad (8)\end{aligned}$$

Denote the constraint function $g(x_0,y_0)$ as follows:

$$g(x_0,y_0)=-x_0^2-(1+y_0)^2(1-\bar{r}_\mathrm{f}^{-2})+2(1-\bar{r}_\mathrm{f}^{-1}). \qquad (9)$$

It can be analytically easily shown by Eq. (5) that $M\subset O$; see also the hodograph plane in Marec (1979) and Fig. 1 in Section 4. Note that in set O, $\Delta v(x_0,y_0)$ and the constraint function $g(x_0,y_0)$ have continuous second-order partial derivatives since the origin is also excluded from O. In addition, point $(0,-1)$ is not in M, which implies that all feasible solutions are regular; i.e., the linear independence hypothesis of $\nabla g(x_0,y_0)$ also holds for any feasible solution. Hence, all the conditions, related to the continuity of second-order partial derivatives and the regularity of a local optimum, are satisfied, for the applications of related results from nonlinear programming.

As usual, we use the Lagrange multiplier method and define the Lagrangian function as follows:

$$\begin{aligned}F(x_0,y_0)=&\Delta v(x_0,y_0)\\&+\lambda\left(-x_0^2-(1+y_0)^2(1-\bar{r}_\mathrm{f}^{-2})+2(1-\bar{r}_\mathrm{f}^{-1})\right). \qquad (10)\end{aligned}$$

In view of the Karush-Kuhn-Tucker conditions, e.g., given by Proposition 3.3.1 in Bertsekas (1999) and Corollary 9.6 in Güler (2010), a local optimum of $\Delta v(x_0,y_0)$ must satisfy the following necessary conditions:

$$\frac{\partial F}{\partial x_0}=\frac{x_0}{\Delta v_0}+\frac{x_0}{\Delta v_\mathrm{f}}-2\lambda x_0=0, \qquad (11)$$

$$\begin{aligned}\frac{\partial F}{\partial y_0}=&\frac{y_0}{\Delta v_0}+\frac{y_0+1-\bar{r}_\mathrm{f}^{-3/2}}{\Delta v_\mathrm{f}}\\&-2\lambda(1+y_0)(1-\bar{r}_\mathrm{f}^{-2})=0, \qquad (12)\end{aligned}$$

$$\lambda\left(-x_0^2-(1+y_0)^2(1-\bar{r}_\mathrm{f}^{-2})+2(1-\bar{r}_\mathrm{f}^{-1})\right)=0, \qquad (13)$$

$$-x_0^2-(1+y_0)^2(1-\bar{r}_\mathrm{f}^{-2})+2(1-\bar{r}_\mathrm{f}^{-1})\leq 0,\lambda\geq 0.$$

To find a local optimal solution, we divide the proof of the first part of this theorem into two cases.

Case 1: If $\lambda = 0$, then due to Eqs. (11) and (12), we have $x_0 = 0$ and

$$\frac{y_0}{\Delta v_0} + \frac{y_0 + 1 - \bar{r}_\mathrm{f}^{-3/2}}{\Delta v_\mathrm{f}} = 0, \tag{14}$$

respectively. We claim that Eq. (14) does not hold because the equality $x_0 = 0$ implies that

$$\frac{y_0}{\Delta v_0} = \frac{y_0}{|y_0|} = \pm 1,$$

which contradicts with

$$1 < \frac{y_0 + 1 - \bar{r}_\mathrm{f}^{-3/2}}{\Delta v_\mathrm{f}} = \frac{y_0 + 1 - \bar{r}_\mathrm{f}^{-3/2}}{\sqrt{\left(y_0 + 1 - \bar{r}_\mathrm{f}^{-3/2}\right)^2 - (\bar{r}_\mathrm{f} - 1)^2(2\bar{r}_\mathrm{f} + 1)\bar{r}_\mathrm{f}^{-3}}},$$

or

$$\frac{y_0 + 1 - \bar{r}_\mathrm{f}^{-3/2}}{\Delta v_\mathrm{f}} < -1.$$

Therefore, Eq. (14) has no solution under the assumption $\lambda = 0$.

Case 2: If $\lambda > 0$, then Eq. (13) yields

$$-x_0^2 - (1 + y_0)^2(1 - \bar{r}_\mathrm{f}^{-2}) + 2(1 - \bar{r}_\mathrm{f}^{-1}) = 0, \tag{15}$$

which together with Eq. (4) leads to $x_\mathrm{f}^2 = 0$. Thus,

$$\Delta v_\mathrm{f} = \sqrt{x_\mathrm{f}^2 + y_\mathrm{f}^2} = \sqrt{y_\mathrm{f}^2} = |y_\mathrm{f}|, \tag{16}$$

and $x_0^2 = -(1 + y_0)^2(1 - \bar{r}_\mathrm{f}^{-2}) + 2(1 - \bar{r}_\mathrm{f}^{-1})$. Then we obtain

$$\begin{aligned}\Delta v_0^2 &= x_0^2 + y_0^2 \\ &= \bar{r}_\mathrm{f}^{-2}(1 + y_0)^2 - (1 + 2y_0) + 2(1 - \bar{r}_\mathrm{f}^{-1}) \\ &= \left(\bar{r}_\mathrm{f}^{-1}(1 + y_0) - \bar{r}_\mathrm{f}\right)^2 + 2(1 + y_0) \\ &\quad - \bar{r}_\mathrm{f}^2 - (1 + 2y_0) + 2(1 - \bar{r}_\mathrm{f}^{-1}) \\ &= \left(\bar{r}_\mathrm{f}^{-1}(1 + y_0) - \bar{r}_\mathrm{f}\right)^2 + 3 - \bar{r}_\mathrm{f}^2 - 2\bar{r}_\mathrm{f}^{-1}. \end{aligned} \tag{17}$$

From Eq. (11), we have

$$\frac{x_0}{\Delta v_0} + \frac{x_0}{\Delta v_\mathrm{f}} - 2\lambda x_0 = 0. \tag{18}$$

We now show that $x_0 = 0$ by contradiction. If $x_0 \neq 0$, then Eq. (18) implies that

$$2\lambda = \frac{1}{\Delta v_0} + \frac{1}{\Delta v_\mathrm{f}}. \tag{19}$$

Substituting Eq. (19) into Eq. (12) gives

$$\begin{aligned}&\frac{y_0}{\Delta v_0} + \frac{y_0 + 1 - \bar{r}_\mathrm{f}^{-3/2}}{\Delta v_\mathrm{f}} \\ &\quad = (1 + y_0)(1 - \bar{r}_\mathrm{f}^{-2})\left(\frac{1}{\Delta v_0} + \frac{1}{\Delta v_\mathrm{f}}\right).\end{aligned}$$

Arranging the above equation and using Eqs. (3) and (16), we obtain

$$\begin{aligned}\frac{y_0 - (1 + y_0)(1 - \bar{r}_\mathrm{f}^{-2})}{\Delta v_0} &= \frac{\bar{r}_\mathrm{f}^{-3/2} - (y_0 + 1)\bar{r}_\mathrm{f}^{-2}}{\Delta v_\mathrm{f}} \\ &= \frac{\bar{r}_\mathrm{f}^{-1/2} - (y_0 + 1)\bar{r}_\mathrm{f}^{-1}}{\Delta v_\mathrm{f}}\bar{r}_\mathrm{f}^{-1} = \frac{y_\mathrm{f}}{|y_\mathrm{f}|}\bar{r}_\mathrm{f}^{-1},\end{aligned}$$

where $y_\mathrm{f} \neq 0$ since we have assumed $v_\mathrm{f} > 0$ and just concluded $x_\mathrm{f} = 0$. By further rearranging the above equation, we have

$$\frac{\bar{r}_\mathrm{f}^{-1}(1 + y_0) - \bar{r}_\mathrm{f}}{\Delta v_0} = \frac{y_\mathrm{f}}{|y_\mathrm{f}|} = \begin{cases} 1, & \text{if } y_\mathrm{f} > 0, \\ -1, & \text{if } y_\mathrm{f} < 0. \end{cases} \tag{20}$$

It is noted that Eq. (17) gives a strict inequality:

$$\begin{aligned}\Delta v_0^2 &= \left(\bar{r}_\mathrm{f}^{-1}(1 + y_0) - \bar{r}_\mathrm{f}\right)^2 + 3 - \bar{r}_\mathrm{f}^2 - 2\bar{r}_\mathrm{f}^{-1} \\ &< \left(\bar{r}_\mathrm{f}^{-1}(1 + y_0) - \bar{r}_\mathrm{f}\right)^2, \end{aligned} \tag{21}$$

where the function $3 - \bar{r}_\mathrm{f}^2 - 2\bar{r}_\mathrm{f}^{-1} < 0$ since it is decreasing with respect to $\bar{r}_\mathrm{f}$ and $\bar{r}_\mathrm{f} > 1$. Hence, Eq. (20) contradicts with inequality (21) and does not hold, which implies that the assumption $\lambda > 0$ and the equality $x_0 \neq 0$ do not hold simultaneously. Therefore, $\lambda > 0$ leads to $x_\mathrm{f} = 0$ and $x_0 = 0$.

Summarizing the two cases above, we now conclude that a local optimal solution to problem (7) must have $\lambda^* > 0$, $x_\mathrm{f}^* = 0$, and $x_0^* = 0$. Here and in the sequel, we use an asterisk to denote an optimal value of variables. Then the corresponding perpendicular component y_0 can be obtained from Eq. (15):

$$y_0^* = \sqrt{\frac{2\bar{r}_\mathrm{f}}{1 + \bar{r}_\mathrm{f}}} - 1, \quad \hat{y}_0^* = -\sqrt{\frac{2\bar{r}_\mathrm{f}}{1 + \bar{r}_\mathrm{f}}} - 1. \tag{22}$$

Substituting them into Eqs. (3) and (12) yields

$$\begin{aligned}
y_{\mathrm{f}}^{*} &= \bar{r}_{\mathrm{f}}^{-1/2}\left(1-\sqrt{\frac{2}{1+\bar{r}_{\mathrm{f}}}}\right),\\
\lambda^{*} &= \frac{1}{2(1+y_0^{*})(1-\bar{r}_{\mathrm{f}}^{-2})}\left(1+\frac{y_0^{*}+1-\bar{r}_{\mathrm{f}}^{-3/2}}{y_{\mathrm{f}}^{*}}\right)>0,\\
\hat{y}_{\mathrm{f}}^{*} &= \bar{r}_{\mathrm{f}}^{-1/2}\left(1+\sqrt{\frac{2}{1+\bar{r}_{\mathrm{f}}}}\right),\\
\hat{\lambda}^{*} &= \frac{1}{2(1+\hat{y}_0^{*})(1-\bar{r}_{\mathrm{f}}^{-2})}\left(1+\frac{\hat{y}_0^{*}+1-\bar{r}_{\mathrm{f}}^{-3/2}}{\hat{y}_f^{*}}\right)>0.
\end{aligned} \tag{23}$$

One can see that there exist two sets of local optimal solutions, one of which (x_0^{*}, y_0^{*}) corresponds to the Hohmann transfer, and its Lagrange multiplier is λ^{*}.

We are now in a position to show that (x_0^{*}, y_0^{*}) with respect to the Hohmann transfer is the global minimum. We first show that (x_0^{*}, y_0^{*}) is a strict local minimum. Theorem 3.11 in Avriel (2003) gives a second-order sufficient condition for a strict local minimum; see also Theorem 6 originally in McCormick (1967), Proposition 3.3.2 in Bertsekas (1999), and Corollary 9.22 in Güler (2010). To apply it, we need to calculate the Hessian matrix of the Lagrangian function F defined by Eq. (10) at (x_0^{*}, y_0^{*}):

$$\nabla^2 F(x_0^{*}, y_0^{*}, \lambda^{*}) = \begin{pmatrix} \dfrac{\partial^2 F}{\partial x_0^2} & \dfrac{\partial^2 F}{\partial x_0 \partial y_0} \\ \dfrac{\partial^2 F}{\partial y_0 \partial x_0} & \dfrac{\partial^2 F}{\partial y_0^2} \end{pmatrix}_{(x_0^{*}, y_0^{*})}.$$

After a straightforward calculation, by Eqs. (11) and (12) and using the fact $x_0^{*}=0$, we have

$$\frac{\partial^2 F}{\partial x_0 \partial y_0}(x_0^{*}, y_0^{*}) = \frac{\partial^2 F}{\partial y_0 \partial x_0}(x_0^{*}, y_0^{*}) = 0,$$

and also

$$\begin{aligned}
\frac{\partial^2 F}{\partial x_0^2}(x_0^{*}, y_0^{*}) &= \frac{1}{y_0^{*}} + \frac{1}{y_{\mathrm{f}}^{*}} - 2\lambda^{*}\\
&= \frac{1+\bar{r}_{\mathrm{f}}^{-1}(1+y_0^{*})}{y_0^{*}(1+y_0^{*})(1+\bar{r}_{\mathrm{f}}^{-1})} > 0,
\end{aligned} \tag{24}$$

$$\begin{aligned}
\frac{\partial^2 F}{\partial y_0^2}(x_0^{*}, y_0^{*}) &= \frac{-b}{\left((y_0^{*}+a)^2-b\right)^{3/2}} - 2\lambda^{*}(1-\bar{r}_{\mathrm{f}}^{-2})\\
&< 0,
\end{aligned}$$

where $a = 1-\bar{r}_{\mathrm{f}}^{-3/2}$, $b = (\bar{r}_{\mathrm{f}}-1)^2(2\bar{r}_{\mathrm{f}}+1)\bar{r}_{\mathrm{f}}^{-3} > 0$. Then one can see that the Hessian matrix is an indefinite matrix. Thus, we cannot use the positive definiteness of the Hessian matrix, that is,

$$\boldsymbol{z}^{\mathrm{T}} \nabla^2 F(x_0^{*}, y_0^{*}, \lambda^{*}) \boldsymbol{z} > 0, \quad \forall \boldsymbol{z} \neq \boldsymbol{0},$$

as a sufficient condition to justify the local minimum of (x_0^{*}, y_0^{*}) as usual. Fortunately, Theorem 3.11 in Avriel (2003) tells us that when $\lambda^{*} > 0$ and the inequality constraint is active, if we use the positive definiteness of the Hessian matrix to justify the local minimum, we need to consider only the positive definiteness of the first block of the Hessian matrix with the non-zero vector $\boldsymbol{z} \neq \boldsymbol{0}$ defined by

$$\boldsymbol{z} \in Z(x_0^{*}, y_0^{*}) = \left\{ \boldsymbol{z} : \boldsymbol{z}^{\mathrm{T}} \nabla g(x_0^{*}, y_0^{*}) = 0 \right\}, \tag{25}$$

where $g(x_0, y_0)$ is the constraint function defined by Eq. (9). With this kind of $\boldsymbol{z}$, if $\boldsymbol{z}^{\mathrm{T}} \nabla^2 F(x_0^{*}, y_0^{*}, \lambda^{*}) \boldsymbol{z} > 0$, then (x_0^{*}, y_0^{*}) is a strict local minimum. Specifically, the vector $\boldsymbol{z}$ defined by the set (25) satisfies

$$\begin{aligned}
&\boldsymbol{z}^{\mathrm{T}} \nabla g(x_0^{*}, y_0^{*})\\
&= \begin{bmatrix} z_1 & z_2 \end{bmatrix} \begin{bmatrix} -2x_0 \\ -2(1+y_0)(1-\bar{r}_{\mathrm{f}}^{-2}) \end{bmatrix}_{(x_0^{*}, y_0^{*})} = 0.
\end{aligned} \tag{26}$$

Note that $x_0^{*}=0$ and $-2(1+y_0^{*})(1-\bar{r}_{\mathrm{f}}^{-2}) \neq 0$. Hence, Eq. (26) implies $z_1 \neq 0$ and $z_2 = 0$. Obviously it follows from Eq. (24) that

$$\begin{aligned}
\begin{bmatrix} z_1 & 0 \end{bmatrix} \nabla^2 F(x_0^{*}, y_0^{*}, \lambda^{*}) \begin{bmatrix} z_1 \\ 0 \end{bmatrix} &= z_1 \frac{\partial^2 F}{\partial x_0^2}(x_0^{*}, y_0^{*}) z_1\\
&> 0.
\end{aligned} \tag{27}$$

Therefore, in light of Theorem 3.11 in Avriel (2003), we can conclude that $(x_0^{*},\ y_0^{*})$ is a strict local minimum. The same argument can be used to show that $(\hat{x}_0^{*}, \hat{y}_0^{*})$ is also a strict local minimum in view of inequality (27). Meanwhile, a straightforward calculation gives

$$\Delta v(x_0^{*}, y_0^{*}) < \Delta v(\hat{x}_0^{*}, \hat{y}_0^{*}). \tag{28}$$

We have shown that the constrained optimization problem (7) has a global minimum by Lemma 1, and also a global minimum is a local minimum; see Bertsekas (1999) for the definitions of global and local minima. Hence, one of these two local minima must be global. Then by inequality (28), the pair (x_0^{*}, y_0^{*}) is a global minimum, and further it is the global minimum due to the uniqueness. This completes the proof of the theorem.

Remark 1 Theorem 1 can be extended to the 3D case; i.e., transfer orbits can be non-coplanar with the initial and final circular orbits. We resolve a velocity impulse vector into radial, transverse, and normal components. Then $\Delta \boldsymbol{V}_0$ and $\Delta \boldsymbol{V}_{\rm f}$ have components $(\Delta X_0, \Delta Y_0, \Delta Z_0)$ and $(\Delta X_{\rm f}, \Delta Y_{\rm f}, \Delta Z_{\rm f})$, respectively. To realize an orbital transfer between two coplanar circular orbits, the velocity of the spacecraft must be equal to $(\Delta X_0, V_0+\Delta Y_0, \Delta Z_0)$ at the time t_0^+ and $(-\Delta X_{\rm f}, V_{\rm f}-\Delta Y_{\rm f}, -\Delta Z_{\rm f})$ at the time $t_{\rm f}^-$. Since a transfer orbit of a spacecraft is a conic section, it follows from the conservation of angular momentum and energy that,

$$\begin{aligned}
&r_0\Delta Z_0 = -r_{\rm f}\Delta Z_{\rm f},\\
&r_0(V_0+\Delta Y_0) = r_{\rm f}(V_{\rm f}-\Delta Y_{\rm f}),\\
&\frac{1}{2}\left[(V_0+\Delta Y_0)^2+\Delta X_0^2+\Delta Z_0^2\right]-\frac{\mu}{r_0}\\
&\quad=\frac{1}{2}\left[(V_{\rm f}-\Delta Y_{\rm f})^2+\Delta X_{\rm f}^2+\Delta Z_{\rm f}^2\right]-\frac{\mu}{r_{\rm f}}.
\end{aligned}$$

By an argument similar to that in Section 2, the characteristic velocity $\Delta \boldsymbol{v}$ can be represented in terms of x_0, y_0, and z_0. A straightforward calculation yields the following constrained optimization problem:

$$\begin{aligned}
&\min_{x_0,y_0,z_0}\ \Delta v(x_0,y_0,z_0)\\
&\text{s.t. } x_0^2+(1+y_0)^2(1-\bar{r}_{\rm f}^{-2})-2(1-\bar{r}_{\rm f}^{-1})\\
&\qquad +z_0^2(1-\bar{r}_{\rm f}^{-2})\geq 0.
\end{aligned}$$

Then the same conclusion as in Theorem 1 with $(x_0^*, z_0^*) = (x_{\rm f}^*, z_{\rm f}^*) = 0$ can be drawn, and the details are omitted.

3 Hohmann transfer as dynamic optimization problems

In this section, the orbital transfer problem is formulated as two optimal control problems of a spacecraft in an inverse square law field, driven by velocity impulses, with boundary and interior point constraints. The calculus of variations is used to solve the resulting constrained optimization problems.

3.1 Problem formulation

Consider the motion of a spacecraft in the inverse square gravitational field, and the state equation is

$$\dot{\boldsymbol{r}} = \boldsymbol{v}, \qquad \dot{\boldsymbol{v}} = -\frac{\mu}{r^3}\boldsymbol{r}, \tag{29}$$

where $\boldsymbol{r}(t)$ is the spacecraft position vector and $\boldsymbol{v}(t)$ its velocity vector. The state vector consists of $\boldsymbol{r}(t)$ and $\boldsymbol{v}(t)$. We use Eq. (29) to describe the state of the transfer orbit, which defines a conic; see Curtis (2014).

Problem 1 Take the initial position and velocity vectors of a spacecraft on the initial circular orbit, $\boldsymbol{r}(t_0)$ and $\boldsymbol{v}(t_0)$. The terminal time t_1 is not specified. Let t_0^+ signify just after t_0 and t_1^- signify just before t_1. During the period from t_0^+ to t_1^-, the state evolves over time according to Eq. (29). To guarantee at time t_1^+, the spacecraft enters the finite circular orbit, we impose the following equality constraints on the final state:

$$\begin{aligned}
g_{r1}(\boldsymbol{r}(t_1^+)) &= \left|\boldsymbol{r}(t_1^+)\right| - r_{\rm f} = 0,\\
g_{v1}(\boldsymbol{v}(t_1^+)) &= \left|\boldsymbol{v}(t_1^+)\right| - v_{\rm f} = 0,\\
g_2(\boldsymbol{r}(t_1^+),\boldsymbol{v}(t_1^+)) &= \boldsymbol{r}(t_1^+)\cdot\boldsymbol{v}(t_1^+) = 0,
\end{aligned} \tag{30}$$

where $v_{\rm f}$ is the orbit velocity of the final circular orbit $v_{\rm f} = \sqrt{\mu/r_{\rm f}}$. Suppose that there are velocity impulses at time instants t_0 and t_1,

$$\boldsymbol{v}(t_i^+) = \boldsymbol{v}(t_i^-) + \Delta \boldsymbol{v}_i, \quad i = 0 \text{ or } 1,$$

where $\boldsymbol{v}(t_0^-) = \boldsymbol{v}(t_0)$. The position vector $\boldsymbol{r}(t)$ is continuous at these instants. The optimal control problem is to design $\Delta \boldsymbol{v}_i$ that minimizes the cost functional:

$$J = |\Delta \boldsymbol{v}_0| + |\Delta \boldsymbol{v}_1|, \tag{31}$$

subject to constraint (30).

In control theory, such an optimal control problem is called an impulse control problem, in which there are state or control jumps. Historically, an optimal problem with the cost functional (31) is also referred to as a minimum-fuel problem; see the classical books Bryson and Ho (1975), Leitmann (1981), and Hull (2003). Problem 1 has been proposed in the free version of a Matlab-based software GPOPS solved by a direct optimization method. Here, we use the indirect method, i.e., the calculus of variations. In the next problem we consider the orbital transfer problem as a dynamic optimization problem with interior point constraints.

Problem 2 Consider a situation similar to that in Problem 1. Let $t_{\rm HT}$ be the Hohmann transfer time. Instead of the unspecified terminal time, here the terminal time instant $t_{\rm f} > t_{\rm HT}$ is given and the time

instant t_1 now is an unspecified interior time instant. Condition (30) becomes a set of interior boundary conditions. The optimal control problem is to design $\Delta\boldsymbol{v}_i$ that minimizes cost functional (31) subject to interior boundary condition (30).

3.2 Two-point boundary conditions for Problem 1

Problem 1 is a constrained optimization problem subject to static and dynamic constraints. We use Lagrange multipliers to convert it into an unconstrained one. Define the augmented cost functional as follows:

$$\begin{aligned}\tilde{J}:=&|\Delta\boldsymbol{v}_0|+|\Delta\boldsymbol{v}_1|\\&+\boldsymbol{q}_{r1}^{\mathrm{T}}\left[\boldsymbol{r}(t_0^+)-\boldsymbol{r}(t_0)\right]+\boldsymbol{q}_{r2}^{\mathrm{T}}\left[\boldsymbol{r}(t_1^+)-\boldsymbol{r}(t_1^-)\right]\\&+\boldsymbol{q}_{v1}^{\mathrm{T}}\left[\boldsymbol{v}(t_0^+)-\boldsymbol{v}(t_0)-\Delta\boldsymbol{v}_0\right]\\&+\boldsymbol{q}_{v2}^{\mathrm{T}}\left[\boldsymbol{v}(t_1^+)-\boldsymbol{v}(t_1^-)-\Delta\boldsymbol{v}_1\right]+\gamma_{r1}g_{r1}(\boldsymbol{r}(t_1^+))\\&+\gamma_{v1}g_{v1}(\boldsymbol{v}(t_1^+))+\gamma_2 g_{r2}(\boldsymbol{r}(t_1^+),\boldsymbol{v}(t_1^+))\\&+\int_{t_0^+}^{t_1^-}\left[\boldsymbol{p}_r^{\mathrm{T}}\left(\boldsymbol{v}-\dot{\boldsymbol{r}}\right)+\boldsymbol{p}_v^{\mathrm{T}}\left(-\frac{\mu}{r^3}\boldsymbol{r}-\dot{\boldsymbol{v}}\right)\right]\mathrm{d}t,\end{aligned}$$

where Lagrange multipliers $\boldsymbol{p}_r$ and $\boldsymbol{p}_v$ are also called costate vectors; in particular, Lawden (1963) termed $-\boldsymbol{p}_v$ the primer vector.

We introduce the Hamiltonian function as

$$H(\boldsymbol{r},\boldsymbol{v},\boldsymbol{p}):=\boldsymbol{p}_r^{\mathrm{T}}\boldsymbol{v}-\boldsymbol{p}_v^{\mathrm{T}}\frac{\mu}{r^3}\boldsymbol{r},\ \boldsymbol{p}=\begin{bmatrix}\boldsymbol{p}_r & \boldsymbol{p}_v\end{bmatrix}^{\mathrm{T}}. \quad (32)$$

By taking into account all perturbations, the first variation of the augmented cost functional is

$$\begin{aligned}\delta\tilde{J}=&\frac{\Delta\boldsymbol{v}_0^{\mathrm{T}}}{|\Delta\boldsymbol{v}_0|}\delta\boldsymbol{v}_0+\frac{\Delta\boldsymbol{v}_1^{\mathrm{T}}}{|\Delta\boldsymbol{v}_1|}\delta\boldsymbol{v}_1+\boldsymbol{q}_{r1}^{\mathrm{T}}\left[\mathrm{d}\boldsymbol{r}(t_0^+)-\mathrm{d}\boldsymbol{r}(t_0^-)\right]\\&+\boldsymbol{q}_{r2}^{\mathrm{T}}\left[\mathrm{d}\boldsymbol{r}(t_1^+)-\mathrm{d}\boldsymbol{r}(t_1^-)\right]\\&+\boldsymbol{q}_{v1}^{\mathrm{T}}\left[\mathrm{d}\boldsymbol{v}(t_0^+)-\mathrm{d}\boldsymbol{v}(t_0^-)-\delta\boldsymbol{v}_0\right]\\&+\boldsymbol{q}_{v2}^{\mathrm{T}}\left[\mathrm{d}\boldsymbol{v}(t_1^+)-\mathrm{d}\boldsymbol{v}(t_1^-)-\delta\boldsymbol{v}_1\right]\\&+\mathrm{d}\boldsymbol{r}^{\mathrm{T}}(t_1^+)\frac{\partial g_{r1}(\boldsymbol{r}(t_1^+))}{\partial\boldsymbol{r}(t_1^+)}\Big|_*\gamma_{r1}\\&+\mathrm{d}\boldsymbol{v}^{\mathrm{T}}(t_1^+)\frac{\partial g_{v1}(\boldsymbol{v}(t_1^+))}{\partial\boldsymbol{v}(t_1^+)}\Big|_*\gamma_{v1}\\&+\mathrm{d}\boldsymbol{r}^{\mathrm{T}}(t_1^+)\frac{\partial g_2(\boldsymbol{r}(t_1^+),\boldsymbol{v}(t_1^+))}{\partial\boldsymbol{r}(t_1^+)}\Big|_*\gamma_2\\&+\mathrm{d}\boldsymbol{v}^{\mathrm{T}}(t_1^+)\frac{\partial g_2(\boldsymbol{r}(t_1^+),\boldsymbol{v}(t_1^+))}{\partial\boldsymbol{v}(t_1^+)}\Big|_*\gamma_2\\&+\left(H_*-\boldsymbol{p}_r^{\mathrm{T}}\dot{\boldsymbol{r}}-\boldsymbol{p}_v^{\mathrm{T}}\dot{\boldsymbol{v}}\right)\Big|_{t_1^{-*}}\delta t_1 \qquad (*)\\&+\boldsymbol{p}_r^{\mathrm{T}}(t_0^+)\delta\boldsymbol{r}(t_0^+)-\boldsymbol{p}_r^{\mathrm{T}}(t_1^{-*})\delta\boldsymbol{r}(t_1^{-*})\\&+\boldsymbol{p}_v^{\mathrm{T}}(t_0^+)\delta\boldsymbol{v}(t_0^+)-\boldsymbol{p}_v^{\mathrm{T}}(t_1^{-*})\delta\boldsymbol{v}(t_1^{-*}) \qquad (**)\\&+\int_{t_0^+}^{t_1^{-*}}\left[\left(\frac{\partial H(\boldsymbol{r},\boldsymbol{v},\boldsymbol{p})}{\partial\boldsymbol{r}}+\dot{\boldsymbol{p}}_r(t)\right)_*^{\mathrm{T}}\delta\boldsymbol{r}\right.\\&\left.+\left(\frac{\partial H(\boldsymbol{r},\boldsymbol{v},\boldsymbol{p})}{\partial\boldsymbol{v}}+\dot{\boldsymbol{p}}_v(t)\right)_*^{\mathrm{T}}\delta\boldsymbol{v}\right]\mathrm{d}t, \qquad (33)\end{aligned}$$

where we use $\mathrm{d}(\cdot)$ to denote the difference between the varied path and the optimal path taking into account the differential change at a time instant, for example,

$$\mathrm{d}\boldsymbol{v}(t_1^+)=\boldsymbol{v}(t_1^+)-\boldsymbol{v}^*(t_1^{+*}),$$

and $\delta(\cdot)$ is the variation (for example, $\delta\boldsymbol{v}(t_1^*)$ is the variation of $\boldsymbol{v}$ as an independent variable at t_1^*). Here, the optimal path and optimal impulse time are indicated by an asterisk. Note that $\mathrm{d}\boldsymbol{r}(t_0^-)=\boldsymbol{0}$, $\mathrm{d}\boldsymbol{v}(t_0^-)=\boldsymbol{0}$ since t_0 is fixed. The parts of $\delta\tilde{J}$ in Eq. (33) marked with asterisks are respectively due to the linear term of

$$\int_{t_1^{-*}}^{t_1^{-*}+\delta t_1}\left(H(\boldsymbol{r},\boldsymbol{v},\boldsymbol{p})-\boldsymbol{p}_r^{\mathrm{T}}\dot{\boldsymbol{r}}-\boldsymbol{p}_v^{\mathrm{T}}\dot{\boldsymbol{v}}\right)\mathrm{d}t$$

and the first term in the right-hand side of the following equation:

$$\int_{t_0^+}^{t_1^{-*}}\boldsymbol{p}_r^{\mathrm{T}}\delta\dot{\boldsymbol{r}}\mathrm{d}t=\boldsymbol{p}_r^{\mathrm{T}}\delta\boldsymbol{r}\Big|_{t_0^+}^{t_1^{-*}}-\int_{t_0^+}^{t_1^{-*}}\dot{\boldsymbol{p}}_r^{\mathrm{T}}\delta\boldsymbol{r}\mathrm{d}t,$$

obtained by integrating by parts. To derive boundary conditions, we next use the following relation:

$$\mathrm{d}\boldsymbol{v}(t_1^-)=\delta\boldsymbol{v}(t_1^{-*})+\dot{\boldsymbol{v}}(t_1^{-*})\delta t_1; \quad (34)$$

see Bryson and Ho (1975) and Longuski et al. (2014).

In view of the necessary condition $\delta\tilde{J}=0$ and the fundamental lemma, we have the costate equations as follows:

$$\dot{\boldsymbol{p}}_r(t)=-\frac{\partial H(\boldsymbol{r},\boldsymbol{v},\boldsymbol{p})}{\partial\boldsymbol{r}},\quad \dot{\boldsymbol{p}}_v(t)=-\frac{\partial H(\boldsymbol{r},\boldsymbol{v},\boldsymbol{p})}{\partial\boldsymbol{v}}. \quad (35)$$

Based on the definition of the Hamiltonian function in Eq. (32), the costate (Eq. (35)) can be rewritten as

$$\dot{\boldsymbol{p}}_r = \frac{\partial}{\partial \boldsymbol{r}}\left(\frac{\mu}{r^3}\boldsymbol{r}\right)\boldsymbol{p}_v = -\frac{\mu}{r^3}\left(\frac{3}{r^2}\boldsymbol{r}\boldsymbol{r}^{\mathrm{T}} - \boldsymbol{I}_{3\times 3}\right)\boldsymbol{p}_v,$$
$$\dot{\boldsymbol{p}}_v = -\boldsymbol{p}_r,$$

where $\boldsymbol{I}_{3\times 3}$ is the 3×3 identity matrix.

Using Eq. (34) and regrouping terms in Eq. (33) yield the following terms or equalities for $\Delta\boldsymbol{v}_0, \Delta\boldsymbol{v}_1$, and $\mathrm{d}\boldsymbol{v}$:

$$\left(\frac{\Delta\boldsymbol{v}_0}{|\Delta\boldsymbol{v}_0|} - \boldsymbol{q}_{v1}\right)^{\mathrm{T}}\Delta\boldsymbol{v}_0, \quad \left(\frac{\Delta\boldsymbol{v}_1}{|\Delta\boldsymbol{v}_1|} - \boldsymbol{q}_{v2}\right)^{\mathrm{T}}\Delta\boldsymbol{v}_1,$$
$$\boldsymbol{q}_{v1}^{\mathrm{T}}\mathrm{d}\boldsymbol{v}(t_0^+) + \boldsymbol{p}_v^{\mathrm{T}}(t_0^+)\delta\boldsymbol{v}(t_0^+) = \left(\boldsymbol{q}_{v1}^{\mathrm{T}} + \boldsymbol{p}_v^{\mathrm{T}}(t_0^+)\right)\mathrm{d}\boldsymbol{v}(t_0^+),$$
$$-\boldsymbol{q}_{v2}^{\mathrm{T}}\mathrm{d}\boldsymbol{v}(t_1^-) - \boldsymbol{p}_v^{\mathrm{T}}(t_1^{-*})\left(\delta\boldsymbol{v}(t_1^{-*}) + \dot{\boldsymbol{v}}(t_1^{-*})\delta t_1\right)$$
$$= -\left(\boldsymbol{q}_{v2}^{\mathrm{T}} + \boldsymbol{p}_v^{\mathrm{T}}(t_1^{-*})\right)\mathrm{d}\boldsymbol{v}(t_1^-),$$
$$\left(\boldsymbol{q}_{v2}^{\mathrm{T}} + \gamma_{v1}\frac{\partial g_{v1}(\boldsymbol{v}(t_1^+))}{\partial \boldsymbol{v}^{\mathrm{T}}(t_1^+)}\Big|_* + \gamma_2\frac{\partial g_2(\boldsymbol{r}(t_1^+),\boldsymbol{v}(t_1^+))}{\partial \boldsymbol{v}^{\mathrm{T}}(t_1^+)}\Big|_*\right)$$
$$\cdot\,\mathrm{d}\boldsymbol{v}(t_1^+). \tag{36}$$

As usual, to assure $\delta\tilde{J} = 0$, we choose Lagrange multipliers to make the coefficients of $\Delta\boldsymbol{v}_0$, $\Delta\boldsymbol{v}_1$, $\mathrm{d}\boldsymbol{v}(t_0^+)$, $\mathrm{d}\boldsymbol{v}(t_1^-)$, and $\mathrm{d}\boldsymbol{v}(t_1^+)$ in Eq. (36) vanish:

$$\boldsymbol{q}_{v1} - \frac{\Delta\boldsymbol{v}_0}{|\Delta\boldsymbol{v}_0|} = \boldsymbol{0}, \quad \boldsymbol{q}_{v2} - \frac{\Delta\boldsymbol{v}_1}{|\Delta\boldsymbol{v}_1|} = \boldsymbol{0},$$
$$\boldsymbol{p}_v(t_0^+) + \boldsymbol{q}_{v1} = \boldsymbol{0}, \quad \boldsymbol{p}_v(t_1^{-*}) + \boldsymbol{q}_{v2} = \boldsymbol{0},$$
$$\boldsymbol{q}_{v2} + \gamma_{v1}\frac{\partial g_{v1}(\boldsymbol{v}(t_1^+))}{\partial \boldsymbol{v}(t_1^+)}\Big|_* + \gamma_2\frac{\partial g_2(\boldsymbol{r}(t_1^+),\boldsymbol{v}(t_1^+))}{\partial \boldsymbol{v}(t_1^+)}\Big|_* = \boldsymbol{0}. \tag{37}$$

Applying an argument similar to above for $\boldsymbol{p}_r$ gives

$$\boldsymbol{p}_r(t_0^+) + \boldsymbol{q}_{r1} = \boldsymbol{0}, \quad \boldsymbol{p}_r(t_1^{-*}) + \boldsymbol{q}_{r2} = \boldsymbol{0},$$
$$\boldsymbol{q}_{r2} + \gamma_{r1}\frac{\partial g_{r1}(\boldsymbol{r}(t_1^+))}{\partial \boldsymbol{r}(t_1^+)}\Big|_* + \gamma_2\frac{\partial g_2(\boldsymbol{r}(t_1^+),\boldsymbol{v}(t_1^+))}{\partial \boldsymbol{r}(t_1^+)}\Big|_* = \boldsymbol{0}. \tag{38}$$

We now choose $H(t_1^{-*})$ to cause the coefficient of δt_1 in Eq. (33) to vanish:

$$H(t_1^{-*}) = \boldsymbol{p}_r^{\mathrm{T}}(t_1^{-*})\boldsymbol{v}(t_1^{-*}) - \boldsymbol{p}_v^{\mathrm{T}}(t_1^{-*})\frac{\mu}{r^3(t_1^{-*})}\boldsymbol{r}(t_1^{-*})$$
$$= 0.$$

Finally, by solving the first and second component equations of the last vector equation in Eq. (37), we obtain the Lagrange multipliers γ_{v1} and γ_2. Then substituting them into the first component equations of the last vector equation in Eq. (38) yields the Lagrangian multiplier γ_{r1}. With these Lagrange multipliers and rearranging the second and third component equations of the last vector equation in Eq. (38), we obtain a boundary value equation denoted by

$$g\left(\boldsymbol{r}(t_1^{+*}),\boldsymbol{v}(t_1^{+*});\boldsymbol{p}_r(t_1^{-*}),\boldsymbol{p}_v(t_1^{-*})\right) = 0.$$

List 1 Two-point boundary conditions for Problem 1:

(1) $\boldsymbol{r}(t_0) - \boldsymbol{r}_0 = \boldsymbol{0}, \quad \boldsymbol{v}(t_0^+) - \boldsymbol{v}(t_0^-) - \Delta\boldsymbol{v}_0 = \boldsymbol{0}$;

(2) $\boldsymbol{p}_v(t_0^+) + \dfrac{\Delta\boldsymbol{v}_0}{|\Delta\boldsymbol{v}_0|} = \boldsymbol{0}, \quad \boldsymbol{p}_v(t_1^-) + \dfrac{\Delta\boldsymbol{v}_1}{|\Delta\boldsymbol{v}_1|} = \boldsymbol{0}$;

(3) $H(t_1^-) = 0$;

(4) $\begin{cases} \left|\boldsymbol{r}(t_1^+)\right| - r_{\mathrm{f}} = 0, \\ \left|\boldsymbol{v}(t_1^+)\right| - v_{\mathrm{f}} = 0, \\ \boldsymbol{r}(t_1^+)\cdot\boldsymbol{v}(t_1^+) = 0; \end{cases}$

(5) $g\left(\boldsymbol{r}(t_1^+),\boldsymbol{v}(t_1^+);\boldsymbol{p}_r(t_1^-),\boldsymbol{p}_v(t_1^-)\right) = 0.$

In summary, a complete list including 19 boundary conditions is shown in List 1 where $\boldsymbol{r}(t_1^+) = \boldsymbol{r}(t_1^-), \boldsymbol{v}(t_1^+) = \boldsymbol{v}(t_1^-) + \Delta\boldsymbol{v}_1$. Note that to simplify notation, the "$*$" symbol which denotes an optimal value has been removed.

3.3 Multi-point boundary conditions for Problem 2

Define the augmented cost functional as follows:

$$\begin{aligned}\tilde{J} :=& |\Delta\boldsymbol{v}_0| + |\Delta\boldsymbol{v}_1| \\ &+ \boldsymbol{q}_{r1}^{\mathrm{T}}\left[\boldsymbol{r}(t_0^+) - \boldsymbol{r}(t_0)\right] + \boldsymbol{q}_{r2}^{\mathrm{T}}\left[\boldsymbol{r}(t_1^+) - \boldsymbol{r}(t_1^-)\right] \\ &+ \boldsymbol{q}_{v1}^{\mathrm{T}}\left[\boldsymbol{v}(t_0^+) - \boldsymbol{v}(t_0) - \Delta\boldsymbol{v}_0\right] \\ &+ \boldsymbol{q}_{v2}^{\mathrm{T}}\left[\boldsymbol{v}(t_1^+) - \boldsymbol{v}(t_1^-) - \Delta\boldsymbol{v}_1\right] + \gamma_{r1}g_{r1}(\boldsymbol{r}(t_1^+)) \\ &+ \gamma_{v1}g_{v1}(\boldsymbol{v}(t_1^+)) + \gamma_2 g_{r2}(\boldsymbol{r}(t_1^+),\boldsymbol{v}(t_1^+)) \\ &+ \int_{t_0^+}^{t_1^-}\left[\boldsymbol{p}_r^{\mathrm{T}}(\boldsymbol{v} - \dot{\boldsymbol{r}}) + \boldsymbol{p}_v^{\mathrm{T}}\left(-\frac{\mu}{r^3}\boldsymbol{r} - \dot{\boldsymbol{v}}\right)\right]\mathrm{d}t \\ &+ \int_{t_1^+}^{t_{\mathrm{f}}}\left[\boldsymbol{p}_r^{\mathrm{T}}(\boldsymbol{v} - \dot{\boldsymbol{r}}) + \boldsymbol{p}_v^{\mathrm{T}}\left(-\frac{\mu}{r^3}\boldsymbol{r} - \dot{\boldsymbol{v}}\right)\right]\mathrm{d}t.\end{aligned}$$

We introduce the Hamiltonian functions for two time sub-intervals $[t_0^+, t_1^-] \cup [t_1^+, t_{\mathrm{f}}]$:

$$H_i(\boldsymbol{r},\boldsymbol{v},\boldsymbol{p}_i) := \boldsymbol{p}_{ri}^{\mathrm{T}}\boldsymbol{v} - \boldsymbol{p}_{vi}^{\mathrm{T}}\frac{\mu}{r^3}\boldsymbol{r},$$
$$\boldsymbol{p}_i = \begin{bmatrix}\boldsymbol{p}_{ri} & \boldsymbol{p}_{vi}\end{bmatrix}^{\mathrm{T}}, \qquad i = 1 \text{ or } 2.$$

A tedious and similar argument as used in Problem 1 can be applied to Problem 2 to derive the costate equations and boundary conditions. The two-phase costate equations are given by

$$\dot{\boldsymbol{p}}_{ri}(t)=-\frac{\partial H_i(\boldsymbol{r},\boldsymbol{v},\boldsymbol{p}_i)}{\partial \boldsymbol{r}},$$
$$\dot{\boldsymbol{p}}_{vi}(t)=-\frac{\partial H_i(\boldsymbol{r},\boldsymbol{v},\boldsymbol{p}_i)}{\partial \boldsymbol{v}},\quad i=1 \text{ or } 2.$$

A complete list for boundary conditions is given in List 2.

List 2 Thirty-one boundary conditions for Problem 2:

$$(1)\begin{cases}\boldsymbol{r}(t_0)-\boldsymbol{r}_0=\boldsymbol{0},\\ \boldsymbol{v}(t_0^-)-\boldsymbol{v}(t_0^+)-\Delta\boldsymbol{v}_0=\boldsymbol{0},\\ \boldsymbol{r}(t_1^-)-\boldsymbol{r}(t_1^+)=\boldsymbol{0},\\ \boldsymbol{v}(t_1^-)-\boldsymbol{v}(t_1^+)-\Delta\boldsymbol{v}_1=\boldsymbol{0};\end{cases}$$

$$(2)\begin{cases}\boldsymbol{p}_{v1}(t_0^+)+\dfrac{\Delta\boldsymbol{v}_0}{|\Delta\boldsymbol{v}_0|}=\boldsymbol{0},\\ \boldsymbol{p}_{v1}(t_1^-)+\dfrac{\Delta\boldsymbol{v}_1}{|\Delta\boldsymbol{v}_1|}=\boldsymbol{0},\\ \boldsymbol{p}_{v2}(t_{\rm f})=\boldsymbol{0},\\ \boldsymbol{p}_{r2}(t_{\rm f})=\boldsymbol{0};\end{cases}$$

$$(3)\ H_1(t_1^-)-H_2(t_1^+)=0 \text{ or } -\boldsymbol{p}_{r1}^{\rm T}(t_1^-)\Delta\boldsymbol{v}_1=0;$$

$$(4)\begin{cases}\left|\boldsymbol{r}(t_1^+)\right|-r_{\rm f}=0,\\ \left|\boldsymbol{v}(t_1^+)\right|-v_{\rm f}=0,\\ \boldsymbol{r}(t_1^+)\cdot\boldsymbol{v}(t_1^+)=0;\end{cases}$$

$$(5)\ g\Big(\boldsymbol{r}(t_1^+),\boldsymbol{v}(t_1^+);\boldsymbol{p}_{r1}(t_1^-),\boldsymbol{p}_{r1}(t_1^+),\boldsymbol{p}_{v1}(t_1^-),\boldsymbol{p}_{v1}(t_1^+)\Big)=0.$$

4 Numerical examples

In this section, we provide numerical examples to validate the theoretical results of this study. We first consider the Hohmann transfer via static optimization presented in Section 2 and then the dynamic optimization method in Section 3. For the latter, we demonstrate that the variational method as an indirect optimization method provides highly accurate solutions by using Matlab boundary value solvers.

4.1 Static optimization

Example 1 Consider the orbital transfer problem of two circular orbits. The altitudes of the initial and final circular orbits are 200 km and 800 km, respectively. Hence, their radii are

$$r_0=\text{Re}+200\,000\text{ m},\quad r_{\rm f}=\text{Re}+800\,000\text{ m},$$

where the Earth's radius Re=6 378 145 m. To compare the accuracy of numerical methods, we next display numbers in long format of Matlab. By Eqs. (22) and (23), the magnitudes of velocity impulses for the Hohmann transfer are

$$\begin{aligned}\Delta Y_0=y_0^*\cdot V_0&=\left(\sqrt{\frac{2\bar{r}_{\rm f}}{1+\bar{r}_{\rm f}}}-1\right)\sqrt{\frac{\mu}{r_0}}\\ &=1.679\,487\,971\,110\,013\text{e+02 m/s},\\ \Delta Y_{\rm f}=y_{\rm f}^*\cdot V_0&=\bar{r}_{\rm f}^{-1/2}\left(1-\sqrt{\frac{2}{1+\bar{r}_{\rm f}}}\right)\sqrt{\frac{\mu}{r_0}}\\ &=1.643\,226\,559\,358\,388\text{e+02 m/s},\end{aligned}$$

where $\bar{r}_{\rm f}=r_{\rm f}/r_0$. The cost function is $\Delta v=\Delta Y_0+\Delta Y_{\rm f}=3.322\,714\,530\,468\,401\text{e+02 m/s}$. Meanwhile, the magnitudes of velocity impulses for the local minimum are given by

$$\begin{aligned}\Delta\hat{Y}_0=\hat{y}_0^*\cdot V_0&=\left(-\sqrt{\frac{2\bar{r}_{\rm f}}{1+\bar{r}_{\rm f}}}-1\right)\sqrt{\frac{\mu}{r_0}}\\ &=-1.573\,645\,419\,952\,013\text{e+04 m/s},\\ \Delta\hat{Y}_{\rm f}=\hat{y}_{\rm f}^*\cdot V_0&=\bar{r}_{\rm f}^{-1/2}\left(1+\sqrt{\frac{2}{1+\bar{r}_{\rm f}}}\right)\sqrt{\frac{\mu}{r_0}}\\ &=1.473\,932\,344\,656\,825\text{e+04 m/s},\end{aligned}$$

which drive the spacecraft in the opposite direction to enter the final orbit. The cost function is $\Delta v=\left|\Delta\hat{Y}_0\right|+\left|\Delta\hat{Y}_{\rm f}\right|=3.047\,577\,764\,608\,838\text{e+04 m/s}$.

The constrained optimization problem (7) can also be numerically solved using the Matlab solver fmincon. Then these two sets of solutions can be numerically found by setting different initial values. Fig. 1b shows the 3D graph of the cost function $\Delta v(x_0,y_0)$, in which the point marked by the lower "∘" corresponding to the Hohmann transfer is the global minimum and the other point is the local minimum. In the hodograph plane of Fig. 1, the global minimum M_0 and the local minimum M_1 are the apsides of the elliptical boundary of the constraint set M.

4.2 Dynamic optimization

The Matlab boundary value solvers bvp4c and bvp5c can deal with multi-point boundary

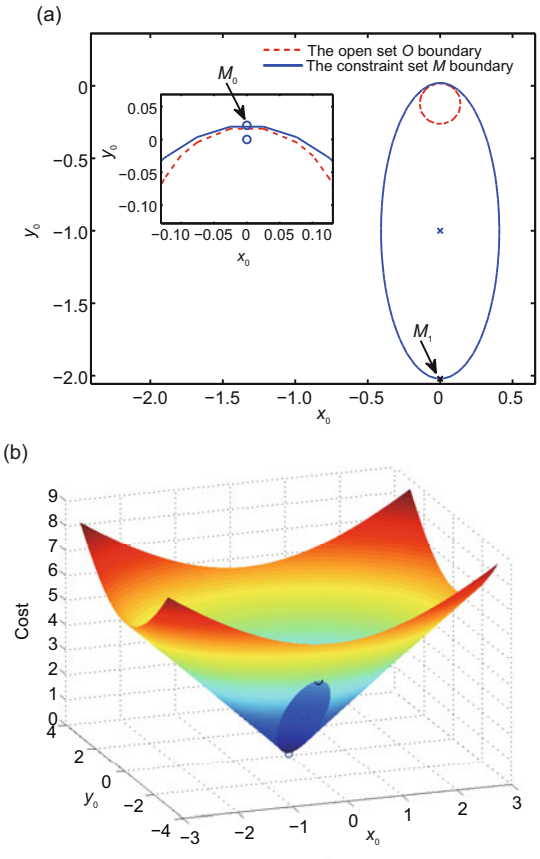

Fig. 1 Hodograph plane (a) and the 3D graph of the cost function $\Delta v(x_0, y_0)$ (b)

value problems with unknown parameters. These two solvers are essentially based on the difference method, collocation, and residual control; see Kierzenka (1998) and Shampine et al. (2003). To use them, we introduce a time change technique. We first consider Problem 2 with an unknown instant t_1. Define a time change

$$\tau = \frac{t - t_0}{t_\mathrm{f} - t_0}, \quad t \in [t_0, t_\mathrm{f}]. \tag{39}$$

Then t_0, t_f, and t_1 are transformed into $0, 1$, and τ_1 $\left(\tau_1 = \dfrac{t_1 - t_0}{t_\mathrm{f} - t_0}\right)$, respectively.

Hence, the time change (Eq. (39)) transforms $[t_0, t_1]$ and $[t_1, t_\mathrm{f}]$ into $[0, \tau_1]$ and $[\tau_1, 1]$, respectively. The non-dimensional factor τ_1 is called a scaled time instant. We now introduce other time changes for each sub-interval:

$$s = \begin{cases} \dfrac{\tau}{2\tau_1}, & \tau \in [0, \tau_1], \\ \dfrac{\tau - 2\tau_1 + 1}{2(1 - \tau_1)}, & \tau \in [\tau_1, 1]. \end{cases} \tag{40}$$

With the time changes (Eqs. (39) and (40)), we have

$$\frac{\mathrm{d}x}{\mathrm{d}t} = \begin{cases} f(x), & t \in [t_0, t_1), \\ f(x), & t \in [t_1, t_\mathrm{f}], \end{cases} \Longrightarrow$$

$$\frac{\mathrm{d}x}{\mathrm{d}s} = \begin{cases} 2\tau_1 t_\mathrm{f} f(x), & s \in [0, 1/2), \\ 2(1 - \tau_1) t_\mathrm{f} f(x), & s \in [1/2, 1]. \end{cases}$$

Therefore, the boundary conditions at t_1 are transformed into the boundary conditions at $1/2$ and so on. Then the Matlab solvers can be used to solve the multi-point boundary value problem of the above piecewise continuous ordinary differential equations (ODEs) with unknown parameters. The number of BCs is the sum of the number of sub-intervals multiplied by the number of equations and the number of unknown parameters. For Problem 1 with an unspecified final time t_f, we need only to nondimensionalize the time:

$$\frac{\mathrm{d}x}{\mathrm{d}t} = f(x), t \in [t_0, t_1] \Longrightarrow \frac{\mathrm{d}x}{\mathrm{d}s} = t_1 f(x),\ s \in [0, 1],$$

where t_1 is an unknown parameter. For time changes, we refer to, e.g., Zefran et al. (1996) and Longuski et al. (2014), for details.

Example 2 Example 1 illustrates that the Hohmann transfer is the solution to Problem 1. The two groups of analytical solutions have been obtained in Example 1. The Hohmann transfer time is given by

$$t_\mathrm{HT} = \frac{\pi}{\sqrt{\mu}} \left(\frac{r_0 + r_1}{2}\right)^{3/2} = 2.838\,495\,539\,521\,862\mathrm{e}{+03}\ \mathrm{s}.$$

By trial and error, this example is successfully solved using bvp4c. The solution message for the Hohmann transfer is shown in Table 1.

Here, we provide the solver with analytical Jacobians and the dynamical equation is vectorized, which dramatically reduces the computation time. Fig. 2 shows the Hohmann transfer orbit and the magnitude of the primer vector, in which the symbol "∘" corresponds to the time instant at which the velocity impulse occurs, the two circles denote the initial circular orbit and the final circular orbit, and between them is the Hohmann transfer orbit. By assuming different initial values of the velocity impulses, the local minimum appears and the message provided by solver bvp4 is shown in Table 2.

Table 1 Solution message for the Hohmann transfer in Example 2

Item	Value
Maximum residual	1.464e–09
Elapsed time	187.023 398 s
First velocity impulse	[0.000 000 000 000 000; 167.948 797 111 000 2; 0]
Second velocity impulse	[0.000 000 000 000 000; –164.322 655 935 838 8; 0]
Time instant of the second velocity impulse	2.838 495 539 521 862e+03
Maximum error of boundary conditions	2.842 171e–14

Table 2 Solution message for the local minimum in Example 2

Item	Value
Maximum residual	1.464e–09
Elapsed time	243.502 088 s
First velocity impulse	[0.000 000 000 000 000; –15 736.454 199 520 13; 0]
Second velocity impulse	[0.000 000 000 000 000; –14 739.323 446 568 25; 0]
Time instant of the second velocity impulse	2.838 495 539 521 862e+03
Maximum error of boundary conditions	1.818 989e–12

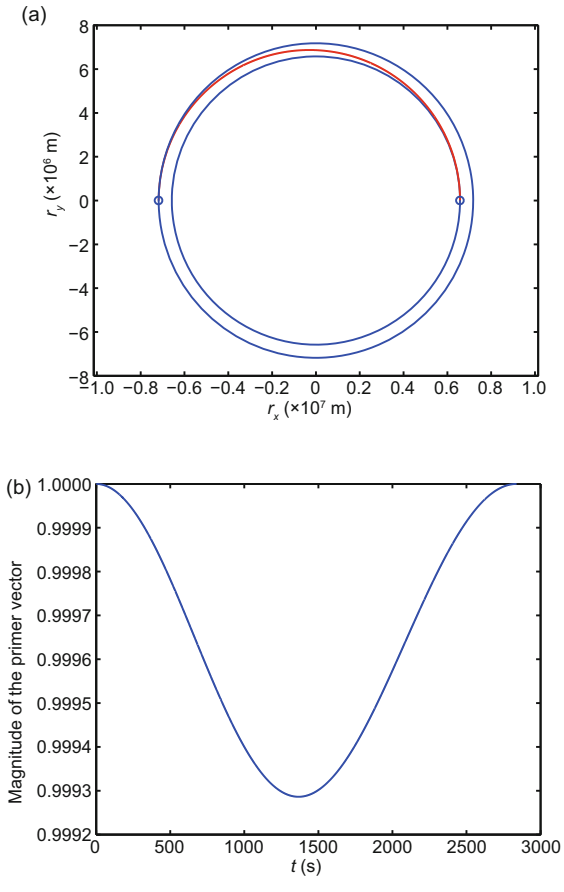

Fig. 2 Hohmann transfer (a) and the magnitude of the primer vector in Example 2 for Problem 1 (b)

This example shows that the variational method as an indirect optimization method provides highly accurate solutions once the solutions are found.

Example 3 Consider the Hohmann transfer as the multi-point boundary value problem (Problem 2). The altitudes of the initial and final circular orbits are 200 km and 400 km, respectively. By the formulas of the Hohmann transfer, the magnitudes of two velocity impulses are given by

$$\Delta v_1 = 58.064\,987\,253\,967\,857,$$
$$\Delta v_2 = 57.631\,827\,424\,189\,602.$$

The Hohmann transfer time is

$$t_{\mathrm{HT}} = 2.715\,594\,949\,192\,177\mathrm{e}+03\ \mathrm{s}.$$

Hence, we choose the terminal time $t_{\mathrm{f}} = 2800$ s. By trial and error, this example is successfully solved by bvp4c, and the solution message is shown in Table 3.

Fig. 3 shows the Hohmann transfer and the magnitude of the primer vector. Fig. 4 is a zoom of the primer vector magnitude, from which one can see that the primer vector achieves its maximum magnitude one at the impulse instants t_0 and t_1. In addition, the discontinuity of the primer vector at t_1 is a supplement to the primer vector theory for the time-open case where the primer vector and its first derivative are continuous everywhere; see Prussing (2010).

By taking different initial values of the velocity impulses, the solution corresponding to the local minimum $(\hat{x}_0^*, \hat{y}_0^*)$ is found by the solver bvp5c. The solution message is shown in Table 4.

Table 3 Solution message for the Hohmann transfer in Example 3

Item	Value
Maximum residual	4.887e–08
Elapsed time	406.320 776 s
First velocity impulse	[0.000 000 000 000 001; 58.064 987 253 970 472; 0]
Second velocity impulse	[0.000 000 000 000 924; –57.631 827 424 187 151; 0]
Scaled instant of the second velocity impulse	0.969 855 338 997 211
Time instant of the second velocity impulse	2.715 594 949 192 190e+03
Maximum error of boundary conditions	4.263 256e–13

Table 4 Solution message for the local minimum in Example 3

Item	Value
Maximum error	5.291e–14
Elapsed time	190.920 474 s
First velocity impulse	[0.000 000 000 000 001; –15 626.570 389 663 10; 0]
Second velocity impulse	[0.000 000 000 000 011; –15 279.466 972 805 44; 0]
Scaled instant of the second velocity impulse	0.969 855 338 997 205
Time instant of the second velocity impulse	2.715 594 949 192 175e+03
Maximum error of boundary conditions	4.403 455e–10

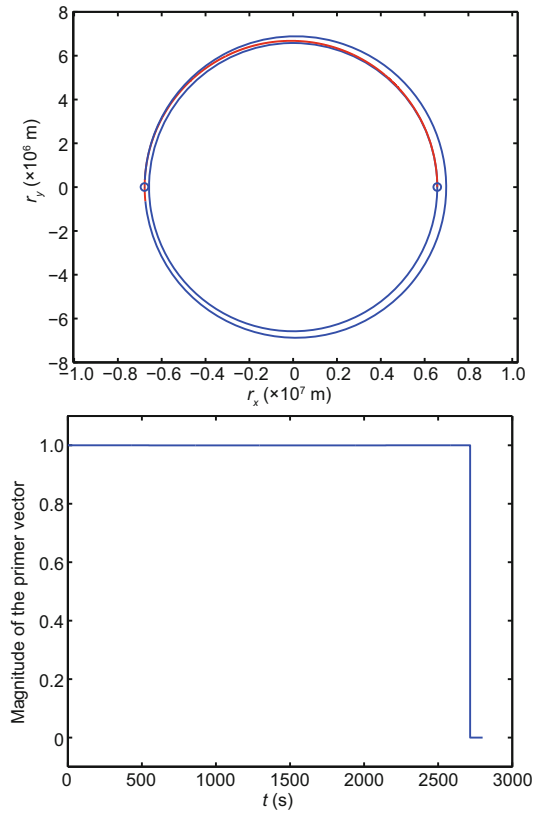

Fig. 3 Hohmann transfer (a) and the magnitude of the primer vector in Example 3 for Problem 2 (b)

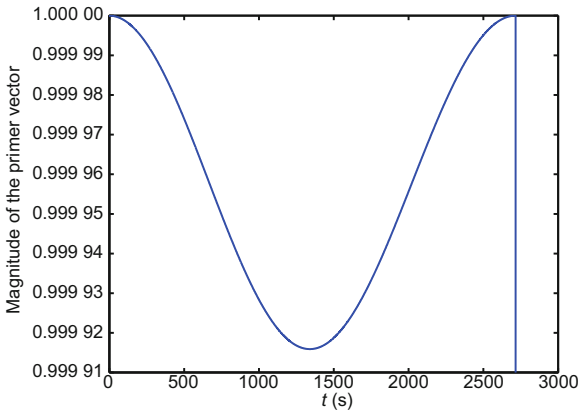

Fig. 4 A zoom of the primer vector magnitude in Example 3

Fig. 5 shows the orbital transfer and the magnitude of the primer vector corresponding to the local minimum $(\hat{x}_0^*, \hat{y}_0^*)$, where the spacecraft starts from the initial point on the initial orbit, moves clockwise along the transfer orbit until the second pulse point, and then travels counterclockwise along the final circular orbit until the terminal point marked with the symbol "×".

5 Conclusions

In this paper, by a static constrained optimization, we have studied the global optimality of the Hohmann transfer using a nonlinear programming method. Specifically, an inequality associated with the conservation of energy has been used to define an inequality constraint. Then we formulated the Hohmann transfer problem as a constrained

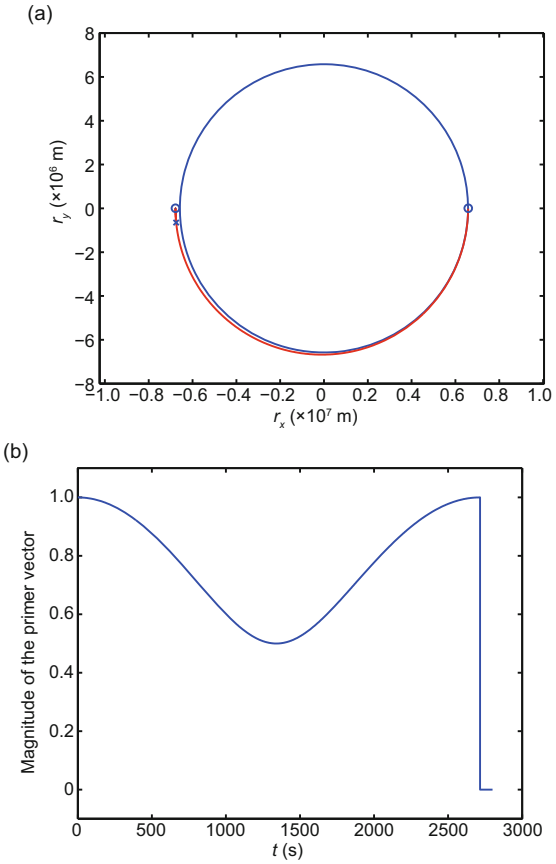

Fig. 5 Orbital transfer (a) and the magnitude of the primer vector corresponding to the local minimum in Example 3 for Problem 2 (b)

nonlinear programming problem. A natural application of the well-known results in nonlinear programming such as the Kuhn-Tucker theorem and a second-order sufficient condition for minima clearly showed the global minimum of the Hohmann transfer. We also have introduced two optimal control problems with two- and multi-point boundary value constraints. With the help of Matlab solvers, the Hohmann transfer and the local minimum were numerically obtained successfully. Numerical examples showed that the variational method as an indirect optimization method can provide highly accurate solutions once the solutions are found.

References

Avendaño M, Martín-Molina V, Martín-Morales J, et al., 2016. Algebraic approach to the minimum-cost multi-impulse orbit-transfer problem. *J Guid Contr Dynam*, 39(8):1734-1743. https://doi.org/10.2514/1.G001598

Avriel M, 2003. Nonlinear Programming: Analysis and Methods. Dover Publications Inc., Mineola, NY, USA.

Barrar RB, 1963. An analytic proof that the Hohmann type transfer is the true minimum two-impulse transfer. *Acta Astronaut*, 9(1):1-11.

Battin RH, 1987. An Introduction to the Mathematics and Methods of Astrodynamics. AIAA, New York, USA.

Bertsekas DP, 1999. Nonlinear Programming (2nd Ed.). Athena Scientific, Belmont, Egypt.

Bryson AEJr, Ho YC, 1975. Applied Optimal Control. Hemisphere Publishing Corp., Washington, USA.

Cornelisse JW, Schöyer HFR, Wakker KF, 1979. Rocket Propulsion and Spaceflight Dynamics. Pitman, London, UK.

Curtis HD, 2014. Orbital Mechanics for Engineering Students. Elsevier, Amsterdam, the Netherlands.

Güler O, 2010. Foundations of Optimization. Springer, New York, USA. https://doi.org/10.1007/978-0-387-68407-9

Gurfil P, Seidelmann PK, 2016. Celestial Mechanics and Astrodynamics: Theory and Practice. Springer Berlin Heidelberg, Germany. https://doi.org/10.1007/978-3-662-50370-6

Hazelrigg GA, 1984. Globally optimal impulsive transfers via Green's theorem. *J Guid Contr Dynam*, 7(4):462-470. https://doi.org/10.2514/3.19879

Hohmann W, 1960. The Attainability of Heavenly Bodies. NASA Technical Translation F-44, Washington, USA.

Hull DG, 2003. Optimal Control Theory for Applications. Springer, New York, USA. https://doi.org/10.1007/978-1-4757-4180-3

Kierzenka J, 1998. Studies in the Numerical Solution of Ordinary Differential Equations. PhD Thesis, Southern Methodist University, Dallas, USA.

Lawden DF, 1963. Optimal Trajectories for Space Navigation. Butterworths, London, UK.

Leitmann G, 1981. The Calculus of Variations and Optimal Control: an Introduction. Springer, New York, USA.

Li DY, Li DZ, 1991. Further discussion on optimal transfer between two circular orbits by dual impulse. *Chin Space Sci Technol*, 12(6):1-10 (in Chinese).

Longuski JM, Guzmán JJ, Prussing JE, 2014. Optimal Control with Aerospace Applications. Springer, New York, USA. https://doi.org/10.1007/978-1-4614-8945-0

Marec JP, 1979. Optimal Space Trajectories. Elsevier, Amsterdam.

Mathwig J, 2004. On Properties of the Hohmann Transfer. MS Thesis, Rice University, Houston, Texas, USA.

McCormick GP, 1967. Second order conditions for constrained minima. *SIAM J Appl Math*, 15(3):641-652. https://doi.org/10.1137/0115056

Miele A, Ciarcià M, Mathwig J, 2004. Reflections on the Hohmann transfer. *J Optim Theory Appl*, 123(2): 233-253. https://doi.org/10.1007/s10957-004-5147-z

Moyer HG, 1965. Minimum impulse coplanar circle-ellipse transfer. *AIAA J*, 3(4):723-726. https://doi.org/10.2514/3.2954

Palmore J, 1984. An elementary proof of the optimality of Hohmann transfers. *J Guid Contr Dynam*, 7(5):629-630. https://doi.org/10.2514/3.56375

Pontani M, 2009. Simple method to determine globally optimal orbital transfers. *J Guid Contr Dynam*, 32(3):899-914. https://doi.org/10.2514/1.38143

Prussing JE, 1992. Simple proof of the global optimality of the Hohmann transfer. *J Guid Contr Dynam*, 15(4):1037-1038. https://doi.org/10.2514/3.20941

Prussing JE, 2010. Primer vector theory and applications. In: Conway BA (Ed.), Spacecraft Trajectory Optimization. Cambridge University Press, Cambridge, p.16-36.

Prussing JE, Conway BA, 1993. Orbital Mechanics. Oxford University Press, New York, USA.

Shampine LF, Gladwell I, Thompson S, 2003. Solving ODEs with Matlab. Cambridge University Press, Cambridge.

Ting L, 1960. Optimum orbital transfer by impulses. *ARS J*, 30(11):1013-1018. https://doi.org/10.2514/8.5305

Vertregt M, 1958. Interplanetary orbits. *J Br Interplanet Soc*, 16:326-354.

Yu ML, 1990. Selection of launch trajectory for launching geosynchronous satellite. *Chin Space Sci Technol*, 2(1):21-27 (in Chinese).

Yuan FY, Matsushima K, 1995. Strong Hohmann transfer theorem. *J Guid Contr Dynam*, 18(2):371-373. https://doi.org/10.2514/3.21394

Zefran M, Desai JP, Kumar V, 1996. Continuous motion plans for robotic systems with changing dynamic behavior. Proc 2nd Int Workshop on Algorithmic Foundations of Robotics.

Zhang G, Zhang XY, Cao XB, 2014. Tangent-impulse transfer from elliptic orbit to an excess velocity vector. *Chin J Aeronaut*, 27(3):577-583. https://doi.org/10.1016/j.cja.2014.04.006